JPC 405

Continuous Measurement of
Solid Propellant Burning Rates

Annual Report

by

J. R. Osborn

R. J. Burick

P. Y. Ho

February 1965

JET PROPULSION CENTER
PURDUE UNIVERSITY

SCHOOL OF MECHANICAL ENGINEERING
LAFAYETTE, INDIANA

CONTINUOUS MEASUREMENT OF SOLID PROPELLANT

BURNING RATES

Annual Report

by

J. R. Osborn

R. J. Burick

P. Y. Ho

Air Force Office of Scientific Research
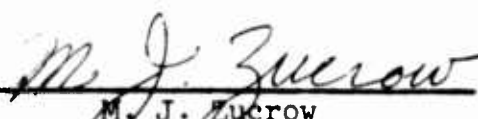
Washington, D. C.

Grant AF-AFOSR 207-64

February 1965

Jet Propulsion Center

Purdue University

Lafayette, Indiana

Approved by: _____

M. J. Zucrow

Atkins Professor of Engineering

ACKNOWLEDGEMENTS

TABLE OF CONTENTS

ABSTRACT

The basic operating principles of an experimental system for the direct and continuous measurement of solid propellant burning rates are presented. The system has been designed and fabricated. Several components of the measurement system have been modified in order to increase the precision of the burning rate measurements.

A continuous burning rate measurement technique, termed the Servo-mechanism Technique, will be employed for obtaining erosive burning rate data for types BDI and BUU double-base propellants. Burning rate measurements will be made with different gas flow velocities parallel to the burning propellant surface; the gas velocities will approach the acoustic speed.

A feasibility study was conducted for determining the adaptability of microwave techniques to the measurement of the burning rate of a solid propellant. It was concluded, because of the dependence of the microwave attenuation upon the combustion conditions present in a research rocket motor, that microwave techniques are not readily adaptable to such burning rate measurements.

A feasibility study indicates that a technique employing ultra-sonic pulses can be developed for obtaining direct measurements of the burning rate of a solid propellant. The technique is based on measuring the time for an ultrasonic pulse to travel through a propellant sample.

INTRODUCTION

Accurate knowledge of the burning rate of a solid propellant is necessary for reducing the costly full scale testing of newly designed solid propellant rocket motors. To date, burning rate theories cannot predict with sufficient accuracy the burning rate characteristics of solid propellants. Consequently, burning rate data which are employed for designing solid propellant rocket engines must be obtained experimentally.

The conventional experimental techniques employed currently for determining the burning rate of a solid propellant often yield erroneous results (1).[1] Several of the indirect measurement techniques utilize some form of probe which is embedded in a propellant sample of propellant grain. Such techniques generally produce inaccurate burning rate data because the high thermal conductivity of the probe increases the rate of heat transfer from the combustion zone to the propellant surface. Furthermore, embedded probes grossly affect the combustion gas flow field adjacent to the burning propellant surface which is undesirable in stu ies concerned with measuring erosive burning rates[2] Direct

---

1. Numbers in parentheses indicate references in the Bibliography.

2. Erosive burning is defined as the change in the linear burning rate due to combustion gas velocity parallel to the burning surface. Linear burning rate is defined as the rate at which the burning surface recedes when there is no combustion gas velocity parallel to the burning surface.

methods of burning rate measurement, such as the photographing of the receding burning surface (2), yield reliable burning rate data and do not disturb the flow field but the reduction of the data is tedious and time consuming. Moreover, available transparent window materials char quickly under high temperature, high gas velocity flow conditions. High temperature gas flows are unavoidable in erosive burning rate experiments, especially in the case of high energy solid propellants.

Investigations at the Jet Propulsion Center, Purdue University, have been concerned with improving the techniques for measuring the burning rates of solid rocket propellants (2),(3,4,5)[3] The subject report presents the recent progress in the aforementioned investigations.

Section II of the subject report is concerned with a burning rate measurement technique which involves a servomechanism, and also discusses a research program based on employing the servomechanism technique for obtaining erosive burning rate data of solid propellants.

Section III of this report discusses the results of a feasibility study for adapting microwave techniques to burning rate measurements.

Section IV discusses a technique for applying ultrasonic waves to the continuous measurement of the burning rate of a solid propellant.

II SERVOMECHANISM MEASUREMENT TECHNIQUE

An experimental system for the direct and continuous measurement of solid propellant burning rates has been developed at the Jet Propulsion Center. A detailed discussion of that technique is presented in References 3, 4, and 5. Only a brief description of that servomechanism technique is presented here.

Figure 1 illustrates schematically the essential features of the servomechanism measurement technique for obtaining the burning rate of a solid propellant. A sample of a solid propellant is bonded to a rectangular holder which is attached to a shaft so that it can move the propellant sample in a linear direction; the holder is incorporated into a two-dimensional research rocket motor. As the solid propellant burns, the burning surface recedes in the direction of its normal with the normal velocity r (6). Simultaneously, the servomechanism moves the propellant sample in the direction opposite to that of the receding burning surface, with the velocity r_s. Thus, if the shaft velocity r_s equals the burning rate, r, the surface of the propellant sample is maintained at a fixed position in the two-dimensional rocket motor.

In that case, the direct measurement of the velocity of the shaft, r_s, yields the instantaneous burning rate of the propellant sample.
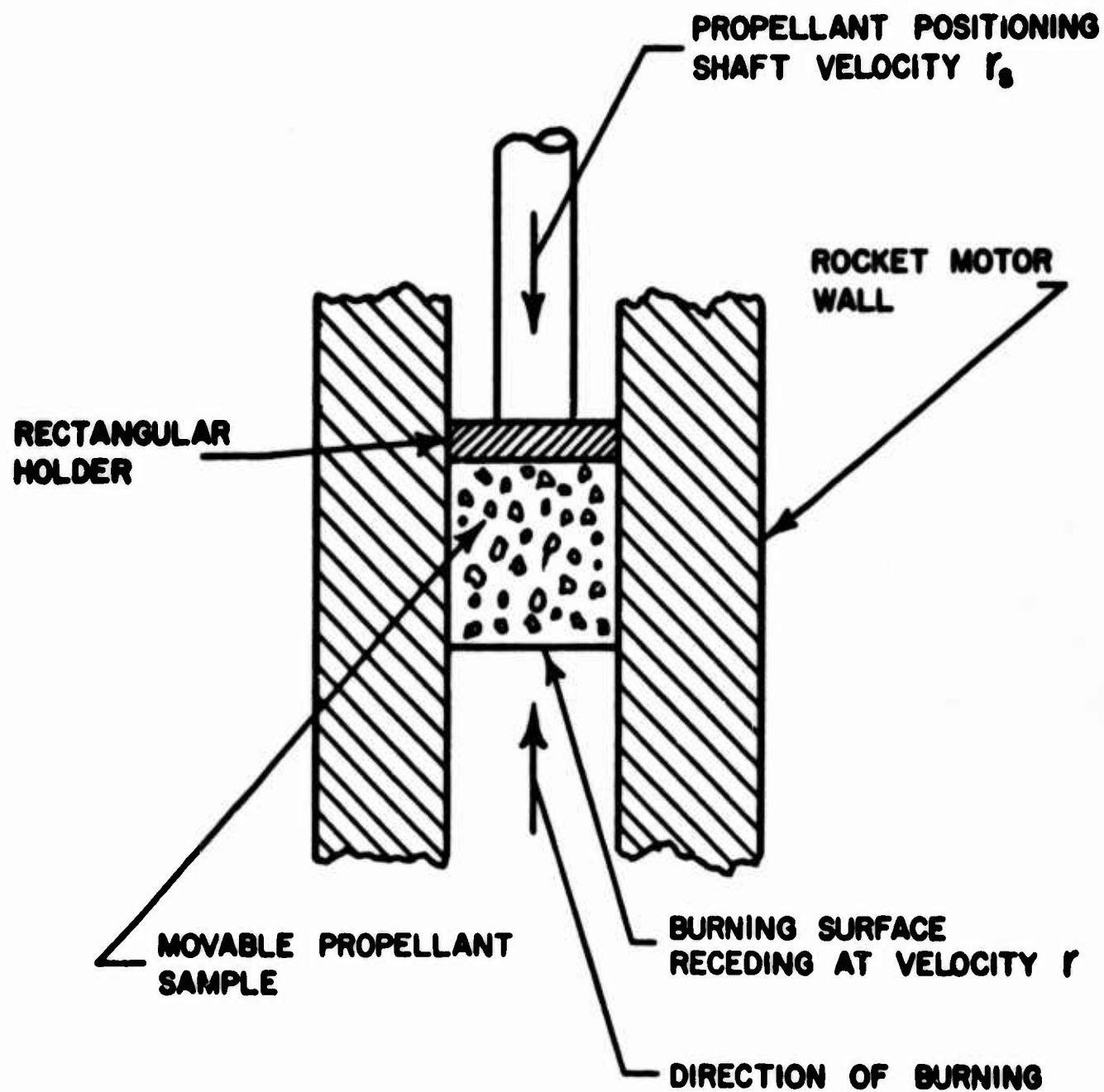
FIG. I   BURNING RATE MEASUREMENT BY THE
SERVOMECHANISM TECHNIQUE

Feedback System

The major problem encountered in developing the aforementioned servomechanism technique was concerned with developing a surface position detector which provides an accurate feedback signal to the servomechanism. Figure 2 presents one successful type of feedback system, the Gamma Ray Feedback System. Another method for providing a feedback signal to the servomechanism is discussed in Section III of this report.

The Gamma Ray Feedback System (see Fig. 2) employs a collimated beam of gamma rays which is attenuated by the propellant sample located inside the two-dimensional rocket motor. The gamma rays are provided by a 125 millicurie source of Cobalt-60. As the propellant burns, the intensity of the collimated beam increases due to the difference in the density of the solid propellant and its combustion products. A scintillation probe measures the change in the intensity of the beam and provides a feedback signal to the servomechanism. The servomechanism then moves the propellant sample to maintain the burning surface at a predetermined position.

To protect personnel from radiation, the radioactive isotope source is surrounded by lead shielding. In addition, the scintillation probe is provided with a lead shield for reducing the background radiation count; a high background radioactive count would produce a feedback signal that is not related to the propellant position.
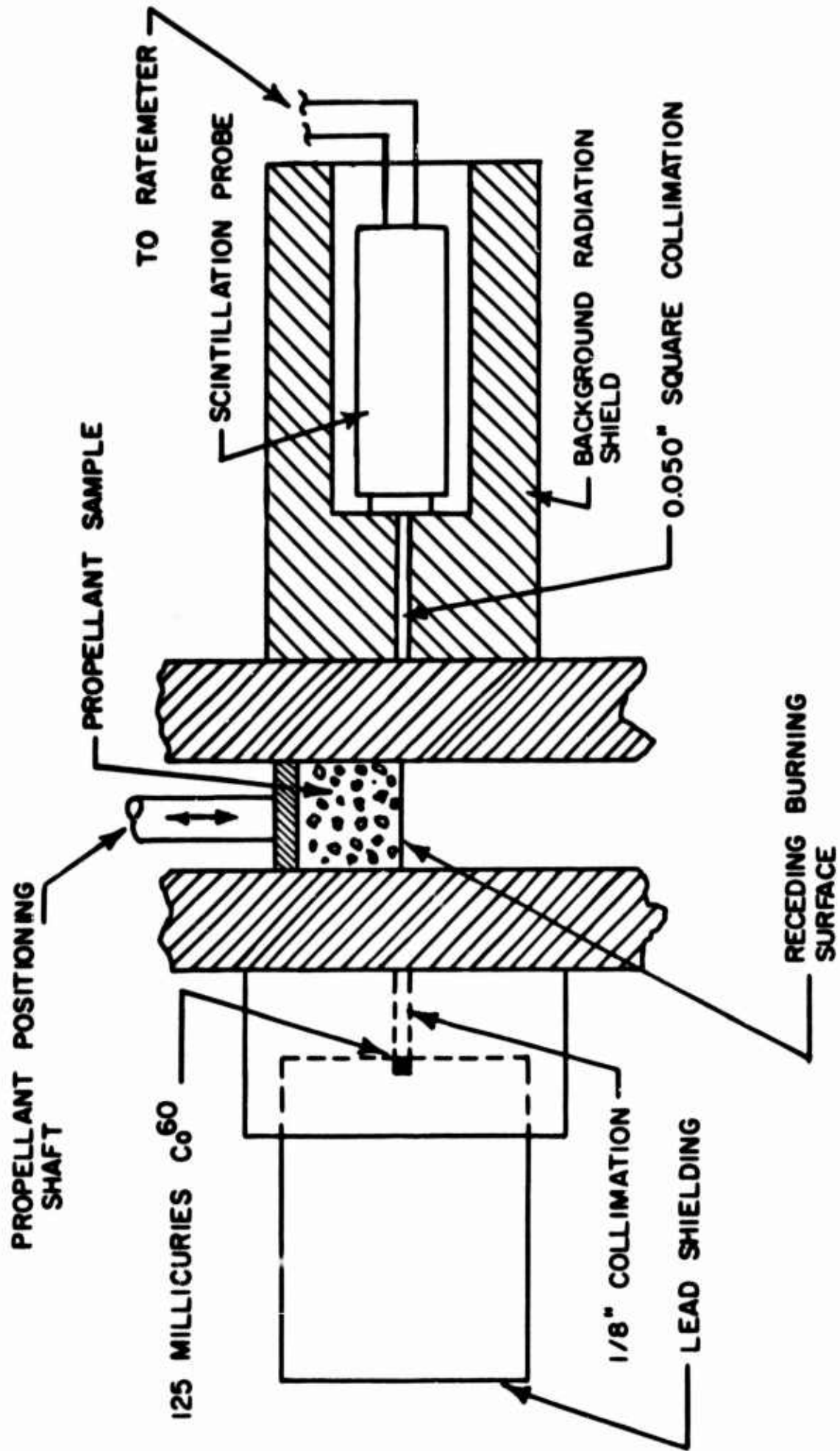
FIG. 2 GAMMA RAY FEEDBACK SYSTEM

Servomechanism System

Figure 3 presents a schematic diagram of the integrated servo-mechanism system. The intensity of the collimated beam of gamma rays is monitored by the scintillation probe which produces a pulsed output. The pulses of the scintillation probe are counted by the ratemeter which converts the count rate to a millivolt signal. The millivolt output of the ratemeter is amplified and subtracted from the reference voltage, and the resulting error signal is amplified by the servo amplifier. The amplified error signal is for exciting the field of the rotating amplifier; the latter is driven at constant speed and produces the power for operating the D. C. servomotor, which operates with a constant field voltage, and the servomotor repositions the propellant sample within the rocket motor.

The burning rate of the propellant is monitored by two separate transducer systems. A linear potentiometer, connected to the shaft which positions the propellant sample within the motor, produces a signal which is proportional to the position of the shaft; the latter is recorded on a direct writing oscillograph, and the slope of the position-time trace is equal to the burning rate of the propellant sample.

The servomotor tachometer coupled with the oscillograph provides a system for monitoring the servomotor speed. Thus, by knowing the gear ratio of the propellant feed mechanism, the burning rate of the propellant sample may be read directly from the oscillogram.
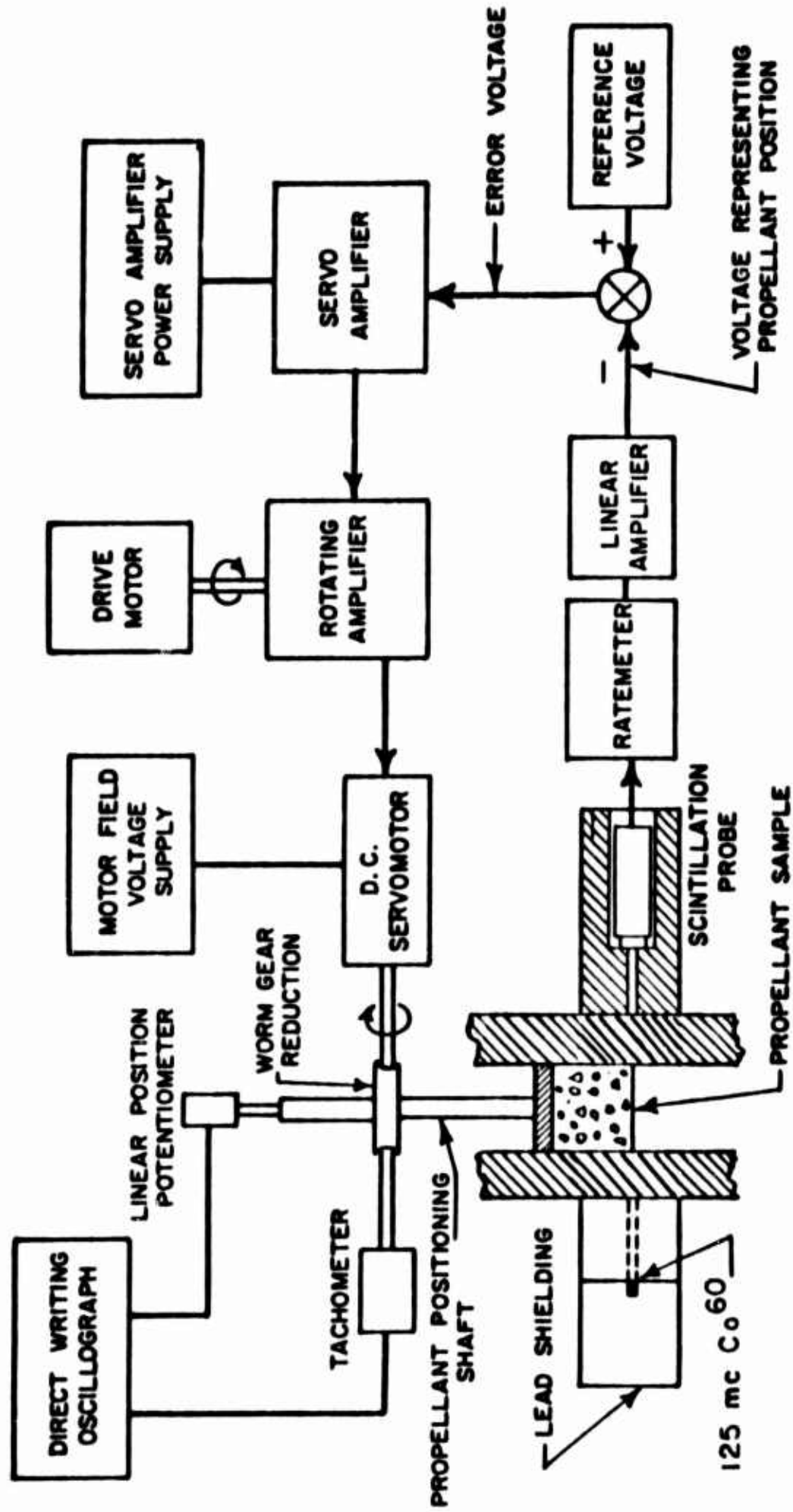
FIG. 3   SERVOMECHANISM SYSTEM

The chamber pressure in the rocket motor is recorded simultaneously with the aforementioned transducer signals. Consequently, at each instant during an experiment the burning rate of the propellant sample can be correlated with the chamber pressure.

Improvement of Servosystem

Propellant Feed Mechanism

As reported in Reference 5, the method for moving the propellant sample within the rocket motor was found to be inadequate under certain operating conditions. At chamber pressures above 400 psi the counter torque which the propellant holder exerted on the propellant position-ing shaft was found to be excessive. Consequently, the propellant holder had a tendency to jam between the sides of the rocket motor causing the servomechanism to become inoperative. The propellant feed mechanism was redesigned to overcome the aforementioned difficulty, and to reduce the friction of the propellant positioning mechanism.

Figure 4 illustrates schematically the redesigned propellant feed mechanism. To provide a torque to counter the friction torque produced by the internally threaded worm gear, a "T" bar was attached to one end of the propellant positioning shaft. The "T" is supported at each end by parallel oil impregnated bronze bars. Thus, as the propellant posi-tioning shaft moves either in a forward or reverse direction the sliding "T" bar provides the necessary counter torque for preventing rotation of the shaft.
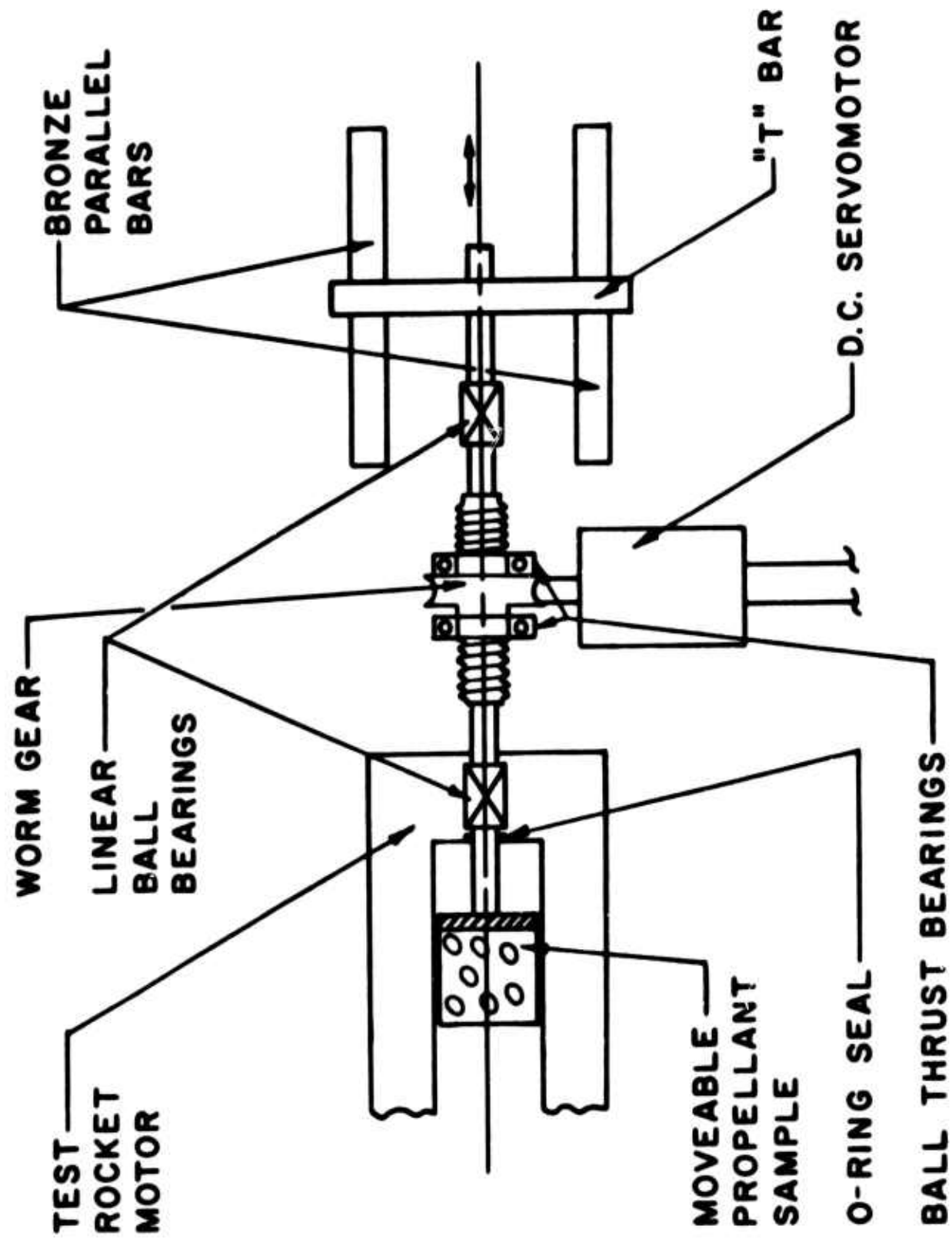
FIG. 4 PROPELLANT FEED MECHANISM

Figure 4 also shows the redesigned bearing system incorporated into the propellant feed mechanism. To reduce shaft friction, linear ball bearings (Thomson Industries) have been installed instead of bronze journal bearings. Furthermore, the bronze thrust bearings employed formerly were replaced by ball thrust bearings.

The redesigned shaft feed mechanism has been tested at chamber pressures in excess of 1,000 psi, and the propellant feed mechanism performed satisfactorily under those conditions.

Isotope Source Strength

The statistical error (root mean square error/count rate) encountered in monitoring the intensity of the collimated gamma ray beam is a function of the counting rate and the time constant of the ratemeter. The net result of the statistical error is a fluctuation in the feedback signal to the servomechanism; the latter can be reduced to a minimum (excluding electronic noise) by either of two means: 1. The time constant of the ratemeter may be increased, or 2. The nominal counting rate at the desired propellant position may be increased by increasing the activity of the isotope source.

Increasing the time constant of the ratemeter to reduce the fluctuations of the feedback signal to the servomechanism results in an overall decrease in the performance of the integrated system. For the subject servomechanism, optimum time constant settings have been found to be 0.1 second or less (4). To reduce the feedback signal fluctuations to an acceptable value (employing a 50 millicurie Cs-137 isotope source) time constants greater than 3.0 seconds are necessary. Thus, since a

3.0 second time constant is detrimental to overall system performance the only alternative to reduce the feedback signal fluctuation was to increase the activity of the isotope source.

The law governing the feedback fluctuations can be expressed, for all practical purposes, by the so-called Poisson error distribution (7). Employing that concept, the feedback signal statistical error encountered in monitoring the collimated beam intensity is given by the following equation. Thus,

$$E = \frac{\sigma}{\bar{n}} = \frac{[\bar{n}]^{1/2}}{\bar{n}} \tag{1}$$

where E is the feedback signal statistical error, σ is the root mean square error, and $\bar{n}$ is the nominal counting rate as indicated by the ratemeter.

As reported in Reference (3), the nominal counting rate when 50 mc of Cs-137 was employed as a source of gamma radiation was 85,000 counts per minute. However, at a ratemeter time constant setting of 0.1 second, 85,000 counts per minute is equivalent to approximately 142 counts per 0.1 second. At that nominal counting rate, an elementary calculation shows the statistical error to be in excess of 8%.

To reduce the statistical error the intensity of the collimated beam was increased to approximately 2.75×10^6 counts per minute, by replacing the 50 mc Cs-137 isotope source by 125 mc of Cobalt-60. Thus, at the optimum ratemeter time constant settings the statistical error is found to be less than 2%.

To monitor the increased intensity of the collimated gamma ray beam it was necessary to replace the original ratemeter (Baird-Atomic Model 432-A) by one having a higher counting rate capability (Baird-Atomic Model Cs-400). With the modified isotope source the servomechanism system has operated satisfactorily.

Erosive Burning Rate Study[4]

The servomechanism technique for measuring the burning rate of a solid propellant is being applied to the investigation of erosive burning characteristics of both double-base and composite solid propellants. A previous erosive burning study at the Jet Propulsion Center employed a photographic technique as the means of obtaining burning rate data (8).

The principal disadvantage of the aforementioned photographic measurement technique was that the reduction of the photographic data is tedious and time consuming. Also, available transparent window materials, with which the research rocket motor was equipped, chared quickly under high temperature, high gas velocity flow conditions. The application of the servomechanism technique for erosive burning rate measurement eliminates the aforementioned disadvantages because the burning rate is recorded directly by an oscillograph, and no windows are needed in the test section of the research rocket motor.

Figure 5 illustrates schematically the experimental apparatus to be employed for obtaining erosive burning rate data. A gas generator will

4. This work will be co-funded by AFOSR under Grant AF-AFOSR 207-64 and by Ballistic Research Laboratories, Aberdeen Proving Grounds, under Contract DA-11-022-AMC-2088(X).

MOVEABLE
PROPELLANT
SAMPLE

REFERENCE PLANE

2-D TEST SECTION

IGNITER

NOZZLE
INSERT

$\leftarrow$ 5.0" $\rightarrow$

U_g

GAS GENERATOR
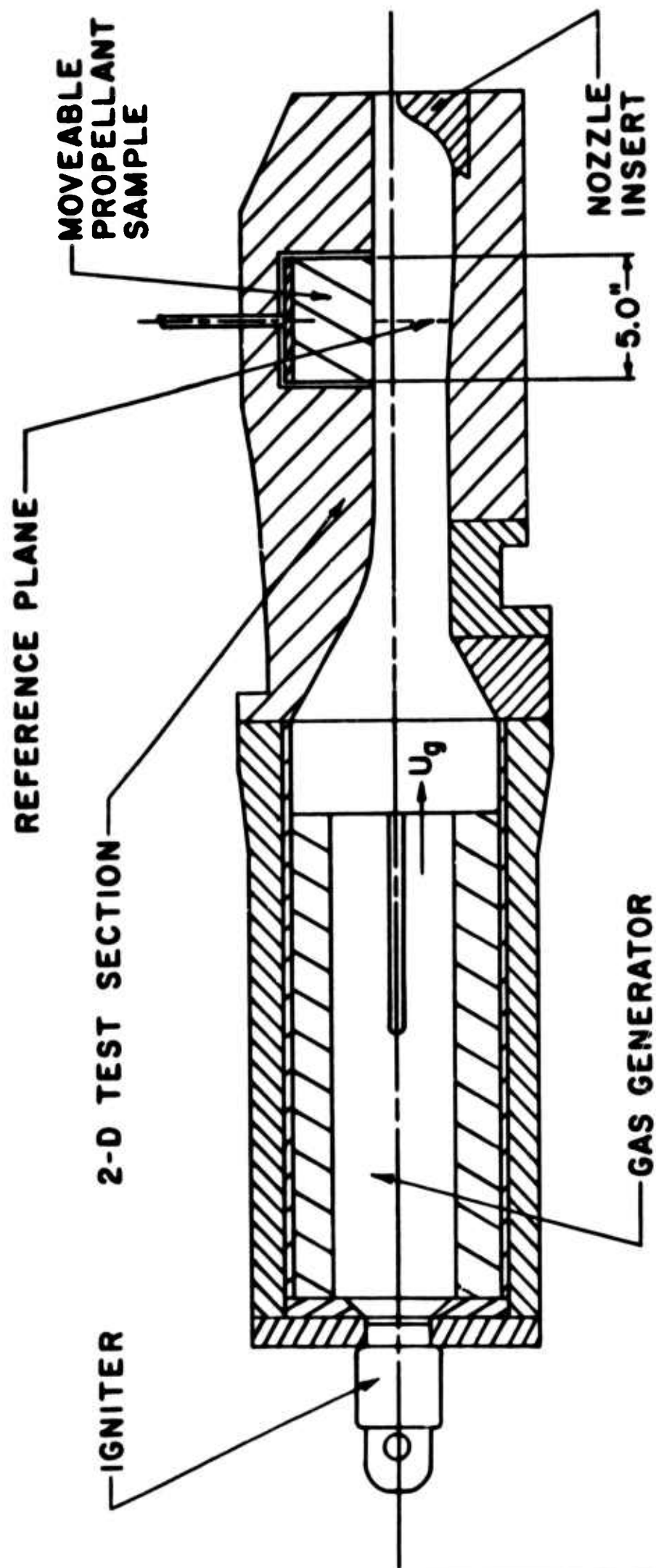
FIG. 5   EROSIVE BURNING RATE APPARATUS

be used to supply hot combustion gases to a two-dimensional test section; the latter will contain a propellant sample which will be moved by the servomechanism at a rate equal to its burning rate. Since one side of the two-dimensional flow channel in the test section will be slightly divergent, the Mach number at any cross-sectional reference plane in the test section will remain constant during the experiment.

The initial erosive burning rate studies will be conducted with types BDI and BUU[5] double-base propellants. Future studies will use double-base and composite propellants with additives such as ballistic modifiers and different percentages of aluminum; in that manner, the effect of the additives upon the erosive burning rate will be determined.

The Mach number of the combustion gases in the reference plane of the test section will be maintained at 0, 0.2, 0.4, 0.6, 0.8, and 0.95 with test section static pressures of 600, 800, 1000, and 1200 psi. The initial temperature of the gas generator propellant and the propellant sample will be -40, 70, and 140°F. It is worth noting that in the past it has been difficult to make erosive burning rate measurements at Mach numbers above 0.6. The servomechanism measurement technique facilitates making measurements at high Mach numbers.

---

5. Complete propellant specifications may be found in the SPIA/M2 Propellant Manual, the Johns Hopkins University, Silver Spring, Maryland, Confidential.

Progress of the Erosive Burning Rate Investigation

Test Facilities

To provide adequate facilities for performing the erosive burning
rate experiments a test cell at the Jet Propulsion Center has been equipped
with the instrumentation for operating the servomechanism system and instru-
mentation for measuring and recording pressures. Included in the instrumenta-
tion are means for the remote operation of high-speed Fastax cameras.

Gas Generator Grain

The design of the gas generating propellant grain has been completed.
Propellant grains and propellant samples for the subject study will be
supplied (GFE) by the Ballistic Research Laboratories, Aberdeen Proving
Ground, Aberdeen, Maryland.

The grain geometry which was chosen for the gas generator is a slotted
tube configuration with two axial slots at the aft end of the grain (9).
The slotted tube configuration which was chosen has the distinct advantage
of an essentially constant mass flow rate (burning area change of less
than 2%) while requiring a simple mandrel configuration.

Igniter

A modified basket type igniter (Aerojet-General, Model CASI-II) will
be used to ignite the gas generating propellant grains. The main charge
of the igniter will consist of approximately 50 grams of ALCID[6] pyrotechnic
pellets and the charge initiater will be a cartridge type squib (Holex
Model 1395). Free volume tests of the igniter are planned in order to
predict approximate igniter performance.

---

6. Trade Name of Aerojet-General Corporation.

III BURNING RATE DETERMINATION BY A
MICROWAVE TECHNIQUE

This section discusses the results of a feasibility study for determining the adaptability of microwave techniques to the measurement of the burning rate of a solid propellant. It should be mentioned at the outset, that currently the complex processes involved in the attenuation of microwaves by solid propellant combustion products are relatively unknown. The analysis which follows is at best a first order approximation to the complex phenomenon of microwave attenuation in solid propellant combustion gases.

Figure 6 illustrates schematically a system for providing a feedback signal to the subject servomechanism. Its operating principle involves passing a microwave beam through the test rocket motor and measuring the change in the effective intensity of the received beam as a function of the position of the movable propellant sample.

The small windows in the sides of the chamber are made of a dielectric material, such as quartz or Plexiglas, which provide a high transmittance for the microwaves. To be capable of predicting the characteristics of the proposed feedback system it is necessary to examine the propagation characteristics of microwaves in the combustion products of the solid propellant sample.
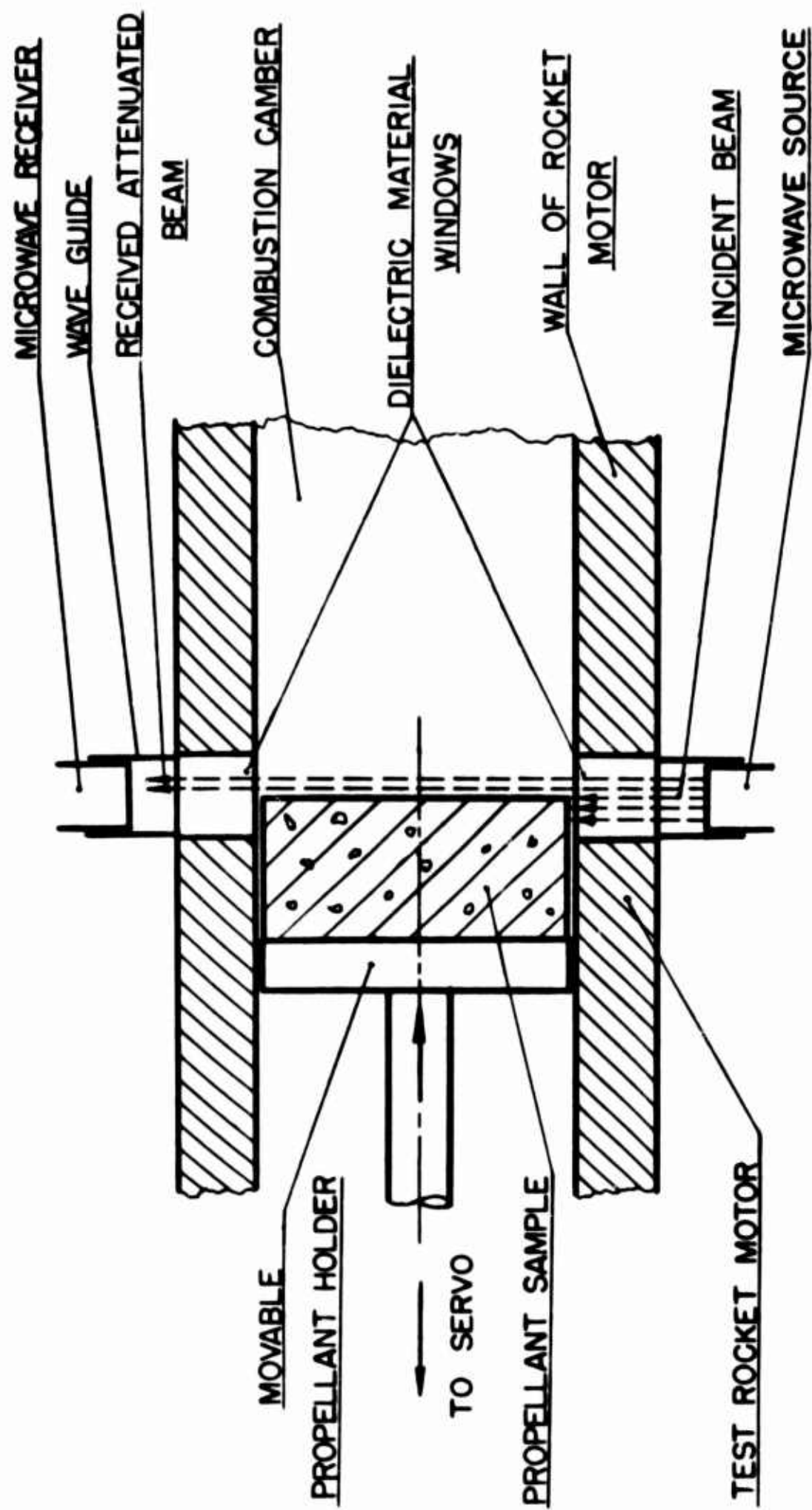
FIG. 6   MICROWAVE TRANSDUCER

The Microwave Equation

A microwave is a type of electromagnetic wave which propagates at the speed of light with frequencies between 1000-300,000 megacycles per second. Its wavelength, however, is longer than that for either ultraviolet, visible, or infrared radiation. Microwaves are emitted and absorbed during the transitions within the molecular rotational spectra; i.e., the low molecular energy levels (10).

The propagation of the microwave can be expressed by the following general form of the wave equation[7]. Thus

$$\nabla (\nabla \cdot \bar{E}) - \nabla^2 \bar{E} = - \mu \frac{\partial \bar{i}}{\partial t} - \mu\epsilon \frac{\partial^2 \bar{E}}{\partial t^2} \qquad (2)$$

where

E = the electric field intensity, volt/m

i = the convective current, coulomb/m^2 sec

μ = the permeability of the medium, henry/m

ϵ = the permissivity of the medium, farad/m = $coulomb^2$/joule m

∇ = the gradient operator, $\bar{i} \frac{\partial}{\partial x} + \bar{j} \frac{\partial}{\partial y} + \bar{k} \frac{\partial}{\partial x}$

Further,

$$\nabla \cdot \bar{i} = - \frac{\partial \rho_e}{\partial t} \qquad (3)$$

where ρ_e is the charge density in coulomb/ft^3. To solve equation 2, it is assumed that the wave is not subjected to attenuation. In that case ρ_e and i both vanish from equation 2. Equation 2 reduces to[8]

$$\nabla^2 \bar{E} = \mu\epsilon \frac{\partial^2 \bar{E}}{\partial t^2} \qquad (4)$$

---

7. A derivation of this general wave equation is presented in Appendix A.

8. Refer to equation 30 in Appendix B. Since $\rho_e = 0$; hence, $\nabla \cdot \bar{E} = 0$.

The solution of equation 4 for a one-dimensional wave propagation is of the form

$$E = A\ e^{j(\omega t - KZ)} + B\ e^{j(\omega t + KZ)} \tag{5}$$

where

A,B   are integration constants to be determined by the appropriate boundary conditions

K   is defined as $K = \omega\sqrt{\mu\epsilon}$, 1/cm

ω is the microwave radian frequency, 1/sec

t   is the time, sec

Z   is the thickness of the combustion chamber, cm

j   is defined as $j = \sqrt{-1}$

If the microwave is propagated one dimensionally along the positive Z coordinate only, the second term in equation 5 can be omitted.

Furthermore, at time equal to zero, and Z equal to zero (the window-gas interface) the electric field intensity is E_o. Considering one-dimensional wave propagation, equation 5 becomes

$$E = E_o\ e^{j(\omega t - KZ)} \tag{6}$$

The attenuation of the microwave is governed by Beer's Law which states that the attenuation of the microwave is an exponential function of the propagation distance Z. Thus,

$$E = E_o\ e^{-\alpha Z}\ e^{j(\omega t - KZ)} \tag{7}$$

where α is an absorption coefficient which is a function of the medium in which the microwave propagates.

The Absorption Coefficient

The absorption coefficient α is a function of several modes of absorption; conductive, molecular, and electronic-transition, and other effects such as ionized combustion gases. The effects of ionized combustion gases are discussed in a later section of this report.

The conductive absorption, α_1, may be found by assuming that the combustion gases are dielectric, and further for simplicity that the charge density is uniform. According to Ohm's- Law

$$\bar{i} = \sigma \bar{E} \tag{8}$$

where σ is the electrical conductivity in mho/meter. Further, considering the conductive absorption only, equation 7 can be rewritten in the form

$$E = E_o \, e^{-\alpha_1 Z} \, e^{j(\omega t - KZ)} \tag{9}$$

where α_1 is the conductive absorption coefficient which is a part of the total absorption coefficient α. Employing equation 8, the first term of equation 2 may be rewritten in the form

$$\nabla (\nabla \cdot \bar{E}) = \nabla \left[\nabla \cdot (\frac{\bar{i}}{\sigma}) \right]$$
$$= \frac{1}{\sigma} \left[\nabla \quad (\nabla \cdot \bar{i}) \right] \tag{10}$$

Combining equation 3 and 10, one obtains

$$\nabla (\nabla \cdot \bar{E}) = \frac{1}{\sigma} \left[\nabla (- \frac{\partial \rho_e}{\partial t}) \right]$$
$$= -\frac{1}{\sigma} \left[\frac{\partial}{\partial t} (\nabla \rho_e) \right]$$
$$= 0$$

since it has been assumed that the charge density is uniform throughout the propagation medium.

Substituting equation 8 into equation 2, and noticing that the first term of equation 2 vanishes, the general wave equation becomes[9]

$$- \nabla^2 E = - \mu \frac{\partial}{\partial t} (\sigma E) - \mu\epsilon \frac{\partial^2 E}{\partial t^2}$$

or

$$\nabla^2 E = \mu \sigma \frac{\partial E}{\partial t} + \mu\epsilon \frac{\partial^2 E}{\partial t^2} \tag{11}$$

Further, utilizing equation 9 and taking its Laplacian, first derivative, and second derivative with respect to time, respectively, one obtains the following three expressions.

$$\nabla^2 E = \frac{\partial^2 E}{\partial^2 z} = (- \alpha_1 - jK)^2 E$$

$$\frac{\partial E}{\partial t} = (j\omega) E$$

$$\frac{\partial^2 E}{\partial t^2} = - \omega^2 E$$

Substituting these expressions into equation 11 yields

$$- (- \alpha_1 - jK)^2 E = - j\omega\mu\sigma E + \omega^2 \mu\epsilon E$$

or

$$(\alpha_1 + jK)^2 = j\omega\mu\sigma - \omega^2 \mu\epsilon$$
$$= j\omega\mu\sigma - K^2$$

---

9. The vector symbols are deleted here since we have assumed one-dimensional propagation of the microwave.

hence,

$$\alpha_1 + jK = \left[-K^2 + j\omega\mu\sigma \right]^{1/2}$$

$$= jK \left[1 - \frac{j\omega\mu\sigma}{K^2} \right]^{1/2}$$

$$= jK \left[1 - \frac{j\omega\mu\sigma}{\omega^2\mu\epsilon} \right]^{1/2}$$

$$= jK \left[1 - \frac{j\sigma}{\omega\epsilon} \right]^{1/2}$$

For a small loss due to dielectric attenuation; i.e., $\frac{\sigma}{\omega\epsilon} \ll 1$, the above relation can be expanded into a Taylor series. Considering only the first term then

$$\alpha_1 + jK = jK \left(1 - \frac{j\sigma}{\omega\epsilon} \right)^{\frac{1}{2}}$$

$$= jK + \frac{\sigma K}{2\omega\epsilon}$$

hence,

$$\alpha_1 = \frac{\sigma K}{2\omega\epsilon}$$

$$= \frac{\sigma\omega\sqrt{\mu\epsilon}}{2\omega\epsilon}$$

or

$$\alpha_1 = \frac{\sigma\sqrt{\frac{\mu}{\epsilon}}}{2} \tag{12}$$

Thus, the conductive absorption coefficient, α_1, is seen to be a function of the electrical conductivity, permeability, and permissivity of the propagation medium.

To illustrate the magnitude of the conductive absorption coefficient, consider the conductive absorption coefficient for air at $2500°K$ and

500 psi: air is considered here because of the lack of data for the electrical conductivity of solid propellant combustion gases. The electrical conductivity of air at these conditions is (11)

$$\sigma = 10^{-4} \qquad mho/cm$$

The permissivity of air, is (12)

$$\epsilon = \frac{1}{36} \cdot 10^{-9} \qquad farad/m$$

The permeability of air, is (12)

$$\mu = 4\pi \cdot 10^{-7} \qquad henry/m$$

Employing equation 12 to calculate the conductive absorption coefficient, one obtains

$$\alpha_1 = \frac{\sigma \sqrt{\frac{\mu}{\epsilon}}}{2} = 0.006 \sqrt{\pi} \qquad cm^{-1}$$

or,

$$\alpha_1 = 0.01064 \qquad cm^{-1}$$

$$\alpha_1 = 0.027 \qquad inch^{-1}$$

Thus, since the attenuation of the microwaves in the combustion gases is a function of $e^{-\alpha z}$ it may be concluded that the attenuation of microwaves by conductive absorption is not the dominant mechanism of attenuation.

To determine the molecular absorption, α_2, that phenomenon must be studied from a microscopic point of view.

Consider a microwave which is incident on a combustion gas molecule. When the microwave collides with the gas molecule, an electron is excited from a quantum state 1 to another quantum state m. Employing the concept of molecular excitation, the molecular absorption coefficient has been shown to be (10)

$$\alpha_{2,i} = \frac{8\pi^3 N}{3000 \ hc} \ f_{lm} \ n_o \ \left|\mu_{lm}\right|^2 \tag{13}$$

where

N = Avogadro's Number,

h = Plaɴch's Constant,

c = the velocity of light,

f_{lm} = the mean frequency of quantum states l and m,

n_o = the molecular concentration,

subscript i refers to the ith molecule in the combustion gases,

and $\left|\mu_{lm}\right|$ is expressed by the integral,

$$\mu_{lm} = \int_{-\infty}^{\infty} L_l \ L_m \ \mu \ dX \tag{14}$$

where

L_l, L_m are the molecular wave functions at states l and m respectively, and

μ = the dipole moment of the molecule.

The evaluation of equation 14 is based on the assumption of the transition of a particle in a box which makes possible the determination of the allowable energies and the position probability function for a particle moving one-dimensionally in a region of length a. Moreover, the wave function is equal to zero at x=0 and x=a. Thus, a is the lowest common multiple of $1/f_l$ and $1/f_m$. The equation for μ_{lm} can be further simplified to (10)

$$\mu_{lm} = \frac{ea}{\pi^2} \ \frac{\cos(l - m) \ \pi - 1}{(l - m)^2} - \frac{\cos(l + m) \ \pi - 1}{(l + m)^2} \tag{15}$$

where e is the electronic change. The molecular absorption follows the
Rules of Section; that is, the transition between energy levels can occur
only if one level has an odd quantum number and the other an even quantum
number, as is shown by equation 15. For example, when $l = 1$, $m = 3$,
equation 15 yields $\mu_{lm} = 0$ and hence $\alpha_2 = 0$. Since the combustion products
are composed of several gaseous species, the molecular absorption for each
species is evaluated by applying equation 15. The summation of the $\alpha_{2,i}$'s
is the molecular absorption coefficient for the combustion products. Thus,
the molecular absorption coefficient is given by

$$\alpha_2 = \sum_{i=1}^{n} \alpha_{2,i} \tag{16}$$

where

α_2 = the molecular absorption coefficient for the combustion products,

$\alpha_{2,i}$ = the molecular absorption coefficient for the ith species of the combustion gas, and

n = the total number of the molecular species in the combustion products.

The molecular absorption coefficient is a function of the combustion
gas temperature and pressure. For different combustion temperatures there
exist different quantum states for transition; hence, f_{lm} and μ_{lm} have
different values. Furthermore, for different combustion gas temperatures
and pressures the molecular concentrations, n_o, is a variable. Consequently,
the molecular absorption coefficients are functions of the propellant
composition as well as the combustion environment.

It is necessary, therefore, to select an optimum microwave frequency for each propellant composition and combustion pressure. The optimum frequency can be determined by using different microwave frequencies through experimental trials, or by analyzing the spectrum of the radiation of the propellant flame which will enable one to select those particular frequencies which are subject to a minimum attenuation.

The absorption due to electronic transition is usually within the region of high frequencies; i.e., in the visible or ultraviolet regions (10). Thus, since the frequencies of the microwave are lower, this mode of absorption can be neglected.

From the foregoing analysis it is concluded that the absorption coefficient, α (see equation 7) is given by

$$\alpha = \alpha_1 + \alpha_2$$

or

$$\alpha = \alpha_1 + \sum_{i=1}^{n} \alpha_{2,i} \tag{17}$$

Although the form of equation 17 is relatively simple, the evaluation of the absorption coefficient α encounters formidable difficulties. Equation 17 requires that the composition of the combustion gases near the burning surface be known. To date, the composition of the combustion above the surface of burning solid propellants cannot be predicted with an accuracy required for determining $\alpha_{2,i}$.

Influence of the Ionized Combustion Gases

The combustion gases in the test rocket motor will, to a certain degree, be ionized (13). Hence, the microwave will be propagated through the slightly ionized gases which will have the characteristics of a plasma. It is to be expected, therefore, that the plasma will block the propagation of the microwave at certain frequencies.

The attenuation of the microwaves by the plasma can be predicted by applying Newton's Law of motion. Thus

$$m \frac{d\overline{V}}{dt} = - \left| e \right| \overline{E} \tag{18}$$

where e is the electronic charge, V is the velocity of the electron, and m is the mass of the electron.

Defining ρ_e as the charge density and assuming the microwave is propagated only in the positive z direction, then

$$i = \rho_e V$$

or

$$V = \frac{i}{\rho_e} = \frac{\sigma}{\rho_e} E \tag{19}$$

In other words, the velocity of the electron, V, is also subject to an exponential attenuation since it is proportional to E at a certain temperature and pressure; hence,

$$\frac{\partial V}{\partial t} = j \omega V$$

$$j \omega V = - \frac{\left| e \right|}{m} E$$

or,

$$V = - \frac{\left|\frac{e}{m}\right| E}{j\omega}$$

thus

$$i = - \frac{\left|\frac{e}{m}\right| \rho_e}{j\omega} E \qquad (20)$$

By assuming uniform ρ_e, the wave equation, equation 2, can be reduced to

$$- (\alpha + jK)^2 E = - \mu \frac{|e|}{m} \rho_e E + \omega^2 \mu\epsilon E$$

or,

$$(\alpha + jK)^2 = - \omega^2 \mu\epsilon + \mu \frac{|e|}{m} \rho_e$$

$$= - \omega^2 \mu\epsilon + \mu\epsilon \omega_p^2$$

where,

$$\omega_p = \left[\frac{|e| \rho_e}{m\epsilon} \right]^{\frac{1}{2}} \qquad (21)$$

Equation 21 defines the so-called radian plasma frequency, 1/sec.

Furthermore,

$$(\alpha + jK)^2 = - \omega^2 \mu\epsilon \left(1 - \frac{\omega_p^2}{\omega^2}\right) \qquad (22)$$

Equation 22 shows that

$$\omega < \omega_p, \quad \alpha + jK = \text{real}$$

or, $\qquad\qquad K = 0$

In that case, the microwave will not pass through the ionized gas.

$$\omega > \omega_p, \quad \alpha + jK = \text{imaginary}$$

or, $\qquad\qquad \alpha = 0$

In the latter case, the microwave will pass through the ionized gas but its phase angle will be altered.

The degree of ionization, $x = n_i/n_o$, can be calculated by the application of the law of mass action and Nernst's heat theorem (14). Thus

$$\frac{x^2}{1-x^2} \ p = 2.4 \times 10^{-4} \ T^{5/2} \ e^{-eV/kT} \tag{23}$$

where

n_i = the ionized molecular concentration of the gas,

n_o = the molecular concentration of the gas,

p = the partial pressure of a gas in mm Hg,

T = the temperature of the gas in ^{o}K,

eV = the electronic potential, and

k = the Boltzman constant.

Further, the charge density ρ_e can be calculated from

$$\rho_e = \rho_o \ \frac{1}{M} \ Ne \tag{24}$$

where

ρ_o = the density of the gas,

M = the molecular weight of the gas,

N = the Avogadro's Number, and

e = the charge of the electron.

As an example, the plasma frequencies for the combustion gases of an Aerojet-General Corp. propellant, ALT 161, is shown in Table 1. The necessary data were taken from Reference 6 and the electronic potential from Reference 14. All data presented in Table 1 are based on a mean combustion pressure of 500 psia and a propellant flame temperature of

Table 1

Gas	Mole Fraction	Partial Pressure	Electronic Voltage (ev)	Degree of Ionization x	Plasma Frequency f (Gc/sec)
H_2	.274	137.0	15.4	1.69×10^{-10}	2.55
H_2O	.099	49.5	12.6	2.19×10^{-8}	18.3
CO_2	0.033	16.5	13.7	6.95×10^{-9}	1.2
N_2	0.001	0.5	15.5	2.54×10^{-9}	15.8 Mc/sec
CO	0.440	220			
KCl	0.151	75.5			
SO_2	0.002	1.0			

An important consideration in adapting a microwave detection system as a servo feedback transducer is that the plasma frequency is a function of the mole fraction, partial pressures, and temperature of the combustion gas. Hence, as the burning rate varies, so does the plasma frequency and accordingly the microwave attenuation. Consequently, a separate microwave transducer calibration system would be required for adapting the transducer to the servomechanism measurement system for each different propellant and combustion pressure.

Conclusions

Based on the foregoing simplified analysis it is concluded that the microwave detection system is not readily adaptable as a feedback transducer for the servomechanism measurement technique, because of the strong dependence of the microwave attenuation upon the combustion conditions in the research rocket motor.

In view of the above, no further work is planned involving the application of the microwave technique to the measurement of the burning rate of a solid propellant.

IV BURNING RATE DETERMINATION BY AN ULTRASONIC TECHNIQUE

This section discusses the use of an ultrasonic technique for determining the burning rate of a solid propellant sample which is located within a research rocket motor. The ultrasonic method under investigation, termed the pulse-echo technique, shows promise as a technique for the continuous measurement of the burning rate of a solid propellant. Before discussing the application of the pulse-echo technique to burning rate measurements a brief discussion will be presented of certain characteristics of ultrasonic wave propagation.

Propagation Characteristics of Ultrasonic Waves

Ultrasonics is a type of sonic pressure wave propagated at frequencies above the audio frequencies of approximately 20 kilocycles per second. The ultrasonic wave is propagated at the speed of sound but with shorter wavelengths. The intensity ratio of the reflected and incident waves at a normal angle of incidence at a boundary between two media can be calculated by (15)

$$\frac{I}{I_1} = \left[\frac{Z_1 - Z_2}{Z_1 + Z_2}\right]^2 \tag{25}$$

where

I, I_1 are the intensities of the reflected and incident waves respectively, and

Z_1, Z_2 are the specific acoustic impedences of media 1 and 2 respectively.

The specific acoustic impedence can be calculated by (15)

$$Z = \rho V \tag{26}$$

where

ρ = the density of the medium, and

V   = the sonic velocity of the wave in the medium.

Table 2 presents the specific acoustic impedence of several media (16).

Table 2

Specific Acoustic Impedence of Several Material

Material	Specific Acoustic Impedence x 10^3 g/cm^2 sec
Aluminum	1690
Carbon Steel	3930
Brass	3610
Plexiglas	320
Porcelain	1290
Synthetic Rubber	140
Glass	1490
Quartz	1440
Water	1490
Air	0.014

Equation 25 can be employed for calculating the percentage of reflected energy between two dissimilar materials. Table 3 presents the calculated results for several materials which are of interest. It is seen from Table 3, that nearly 100% of an incident ultrasonic wave is reflected at a gas-solid interface.

Table 3

Percentages of Reflected Energy at the

Interface of Two Different Materials

Medium I	Medium II	$\dfrac{I_{\curlywedge}}{I_1}$ %
	Synthetic Rubber	86.714
	Glass	20.267
Steel		
	Water	20.267
	Air	99.996
	Glass	68.595
Synthetic Rubber		
	Water	68.595
	Air	99.883
	Water	0
Glass		
	Air	99.989
Water	Air	99.989

Attenuation of an Ultrasonic Wave

The overall attenuation of an ultrasonic wave in a solid is a complex
phenomenon which depends on such factors as bond breaking, scattering,
and thermal conduction of the crystals or particles of the medium. Because
of the aforementioned factor the attenuation phenomenon results in an
exponential decay of the wave intensity as it propagates in a medium.

Furthermore, with each propagation medium there is associated a characteristic decay constant, α. Thus

$$I_x = I_o\ e^{-\alpha x} \tag{27}$$

where

I_x is the attenuated intensity of the ultrasonic wave at distance x from the origin, and

I_o is the intensity of the ultrasonic wave at the origin.

The absorption coefficient, α, is especially large when the mean dimension of the small crystals of the medium is of the order of a wavelength (16). For the majority of solids and metals the damping of sound may be determined by the following equation (16). Thus

$$\alpha = Af + Bf^4 \tag{28}$$

where A and B are empirical determined proportionality constants. The first term in equation 28 predominates in the majority of solids at low frequencies and is due to the presence of elastic hysteresis, the second term accounts for the scattering of sound energy by fine particles. A complete discussion of the frequency dependence of the absorption upon the wavelength and crystal dimensions may be found in References 16, 17.

Ultrasonic Method of Burning Rate Measurement

The relative position of the receding burning surface of a solid propellant sample may be determined in general by three different methods: 1. attenuation measurements, 2. resonance measurements, and 3. pulse-echo measurements. Further, the experimenter has the choice of either propagating the ultrasonic wave through the combustion gases or

through the solid propellant sample. However, the measurement of either the intensity or the propagation of ultrasonic waves in the combustion gas will be affected if acoustic resonance is present in the research rocket motor (18). In addition, the acoustic waves produced by the exhaust nozzle will cause experimental errors. Thus, if the wave is propagated through the solid propellant sample and not through its combustion products the wave will not be subject to the acoustic field of the research rocket motor (refer to Table 3).

Attenuation Measurements

The thickness, and consequently the burning rate, of a solid propellant sample as a function of time may be measured by measuring the relative intensity (wave magnitude) of the reflected and incident waves as predicted by equation 27. However, experiments by Redwood (19) have indicated that the exponential decay of an ultrasonic wave is subject to significant distortions.

The distortion of the exponential decay may originate from propellant surfaces which are not parallel, from interferences between modes of propagation, from non-uniform films which are employed to couple the transducer to the specimen, and from the unequal stressing of a specimen due to thermal gradients. Since such effects may be present in a burning propellant sample the determination of the position of the burning propellant surface by intensity measurement would be subject to significant errors.

Resonance Measurements

The resonance method of determining the position of the burning
surface of a solid propellant sample involves sending a continuous
ultrasonic wave through the propellant sample. A resonance of the
reflected and incident wave is obtained when the thickness of the pro-
pellant sample is an integral number of half wavelengths. However, in
order to obtain a large number of resonances for a small variation in
the sample thickness the wavelength must be small (i.e. the frequency
must be high). At high frequencies the determination of the resonances
in a medium is difficult because of harmonic resonances and highly damped
resonance regions. Thus, the resonance method is not an attractive method
for burning rate measurements.

Pulse-Echo Measurements

Figure 7 illustrates schematically the pulse-echo technique for
direct burning rate measurement of a solid propellant sample. The
technique involves measuring the time required for sonic pulse to travel
from the transducer to the burning surface and then back (the echo) to
the transducer. The input pulse, the echo pulse, and the time elapse
between the two pulses can either be displayed by an oscilloscope or
recorded by an oscillograph.

As shown in Fig. 7, a time delay spacer which has a specific
acoustic impedence similar to that of the propellant, is inserted between
the ultrasonic transducer and the propellant sample. The function of the
spacer is to increase the elapsed time between the pulse and its echo,
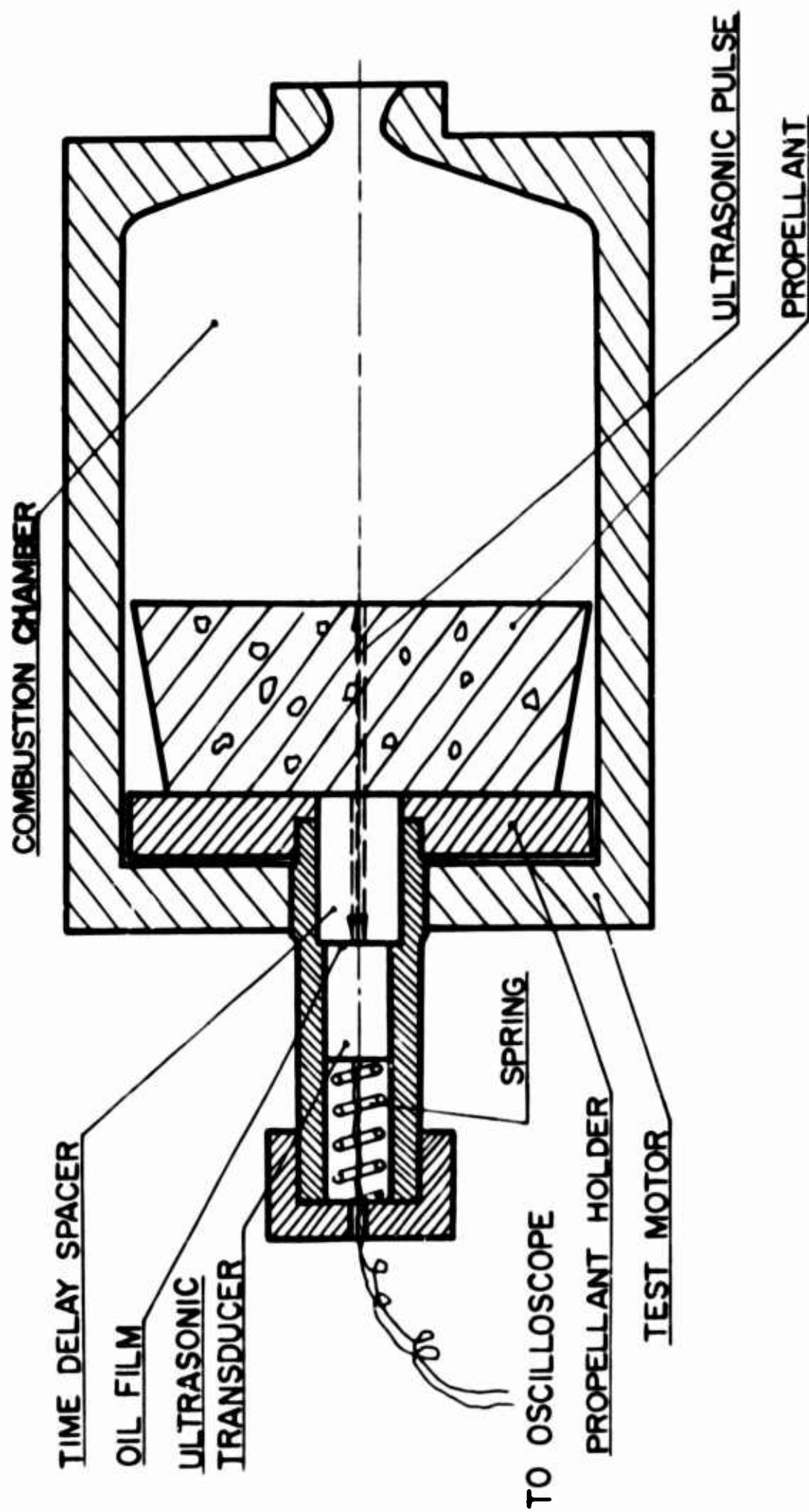thereby raising the precision and the accuracy of the measurement.

COMBUSTION CHAMBER

ULTRASONIC PULSE

PROPELLANT

TIME DELAY SPACER

OIL FILM

ULTRASONIC TRANSDUCER

SPRING

TO OSCILLOSCOPE

PROPELLANT HOLDER

TEST MOTOR

FIG. 7   PULSE-ECHO MEASUREMENT TECHNIQUE

The spacer will also protect the ultrasonic transducer from the high temperatures that occur as the burning surface approaches the transducer.

A thin film of oil is to be applied to the interface of the ultrasonic transducer and the time delay spacer to ensure a region of high transmissivity. The propellant sample will be bonded to the time delay spacer and the propellant holder.

Figure 8 presents the block diagram of such a system. A pulse from the pulse generator propagates to the ultrasonic transducer and is simultaneously recorded by an oscillograph and displayed by an oscilloscope. The ultrasonic pulse wave travels through the propellant sample and is reflected at the burning surface, and the reflected wave then travels back to the transducer, which also functions as an ultrasonic detector. A part of the energy, however, is again reflected at that interface and thus multiple reflection occurs. Consequently, the transducer receives not only the desired reflected wave but also the multi-reflected waves and the waves reflected by the sides of the propellant sample. But the amplitude of the multi-reflected waves will be subject to attenuation in the propellant sample. By proper design, a Schmitt trigger apparatus may be employed for discriminating between the first wave reflection and the multi-reflected waves.

Figure 9 presents the output of the ultrasonic transducer as displayed by an oscilloscope. The trigger level is so chosen such that only the amplitude of the input pulse and its first reflection are above the triggering level. The input pulse and its reflection are then recorded by an oscillograph. Since the speed of the oscillograph and the
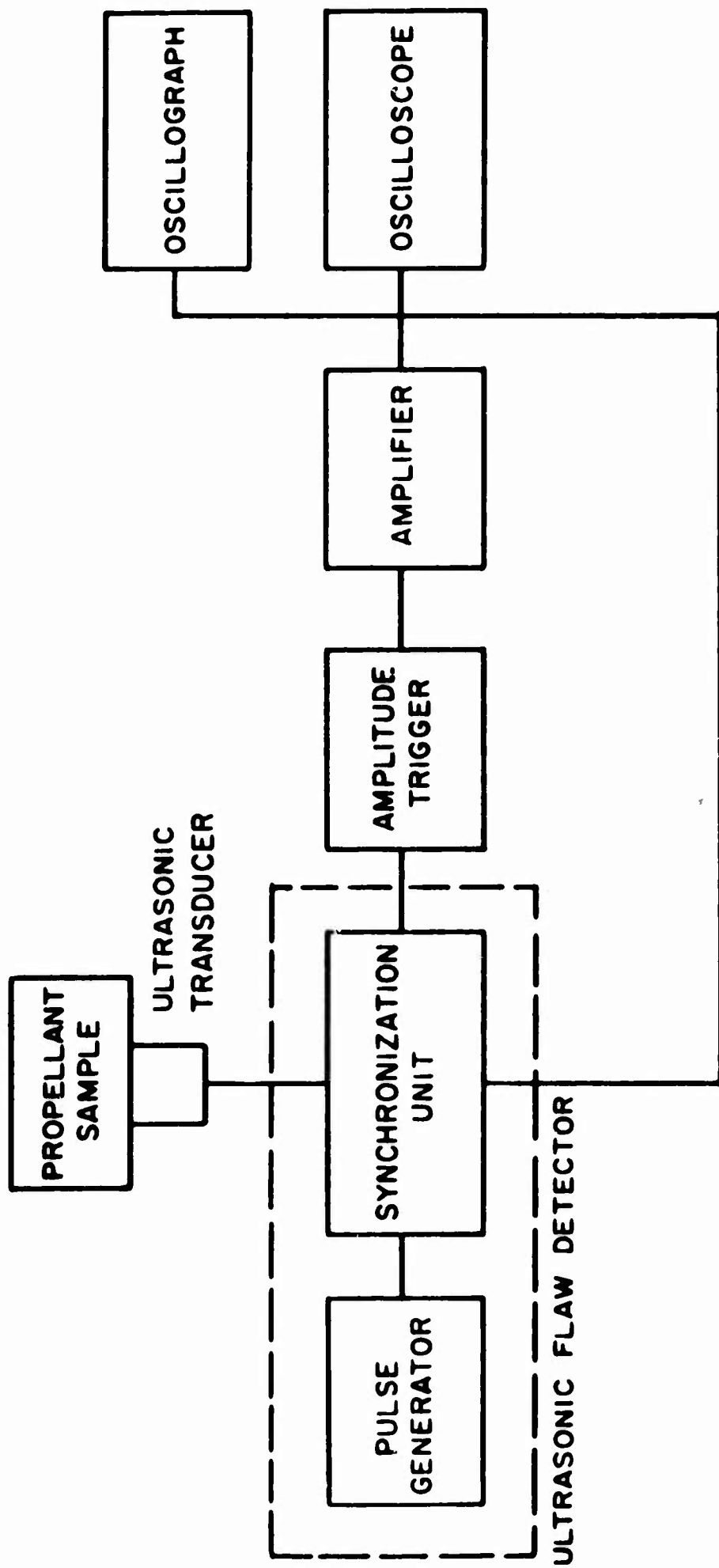
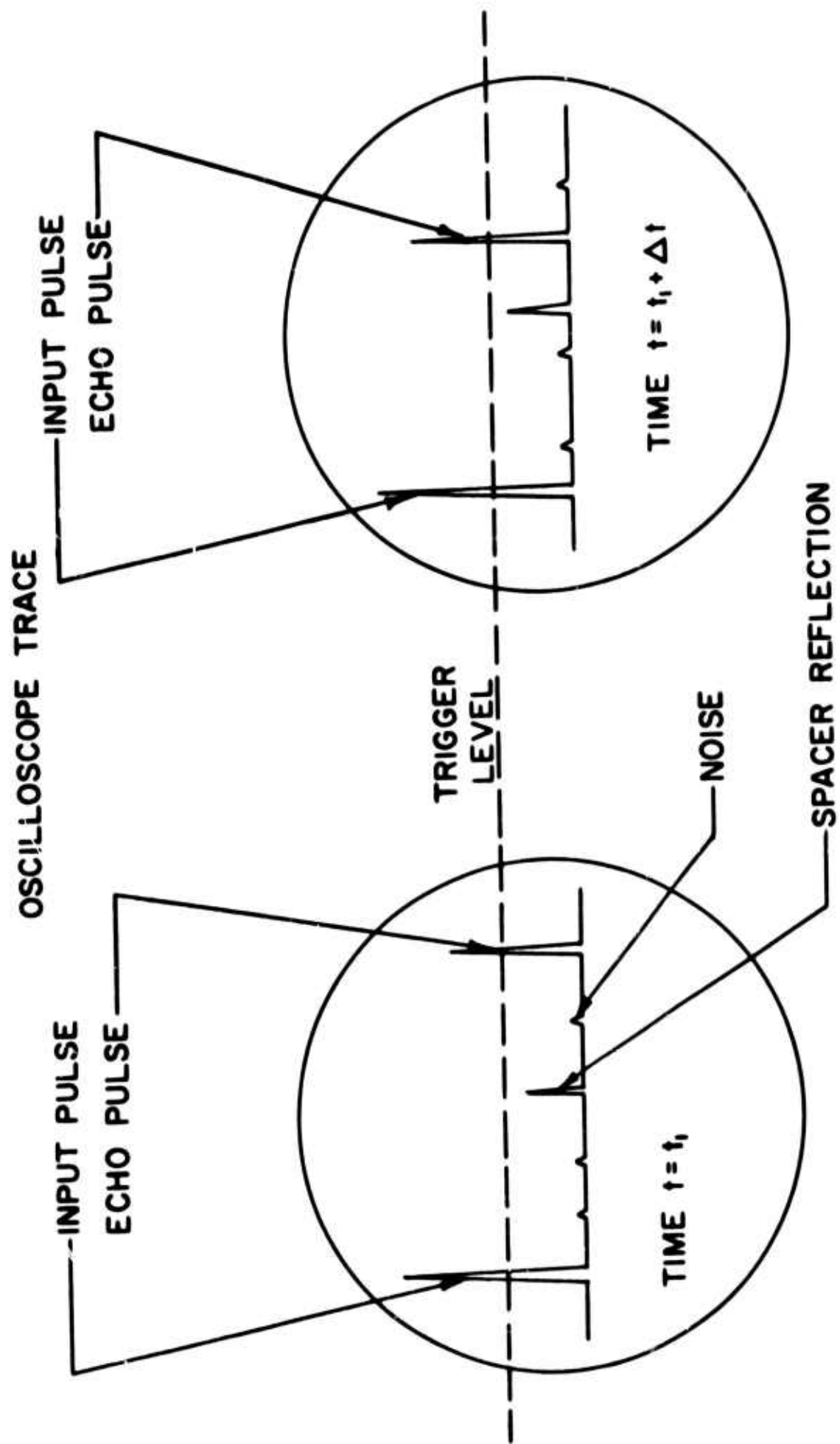FIG. 8   BLOCK DIAGRAM OF THE ULTRASONIC SYSTEM

FIG. 9   ULTRASONIC TRANSDUCER OUTPUT

time sweep of the oscillograph are known, the span between these two
pulses is directly proportional to the travel time of the pulse. By
knowing the propagation velocity of the ultrasonic wave in the propel-
lant sample, the burning rate can be calculated by the following
equation. Thus

$$r = f \, \Delta s = f \, V \frac{\Delta t}{2} = \frac{1}{2} \, fV \frac{\Delta L}{C} \tag{29}$$

where

f = the repetition rate of the generated pulse in cps,

Δs = the thickness change during the time interval in inches,

V = the propagation velocity in in/sec.,

Δt = the traveling time, in sec.,

ΔL = the difference in the pulse-echo spans of two successive input pulses, and

C = the recording speed in in/sec.

A Modification of the Ultrasonic System

A possible modification of this system would be to use a ramp unit,
as shown in Fig. 10, for measuring the traveling time of the reflected
wave. The ramp function, i.e., a voltage having a value which increases
linearly with time, is started at the same time that the input pulse is
generated. The voltage increases linearly until it is stopped by the
echo pulse. For each interval of time between the input and the echo
pulse, the peak voltage will be a direct measurement of the time interval,
and the latter can be converted to a voltage output with respect to the
time. The time interval, which is proportional to the burning rate, may
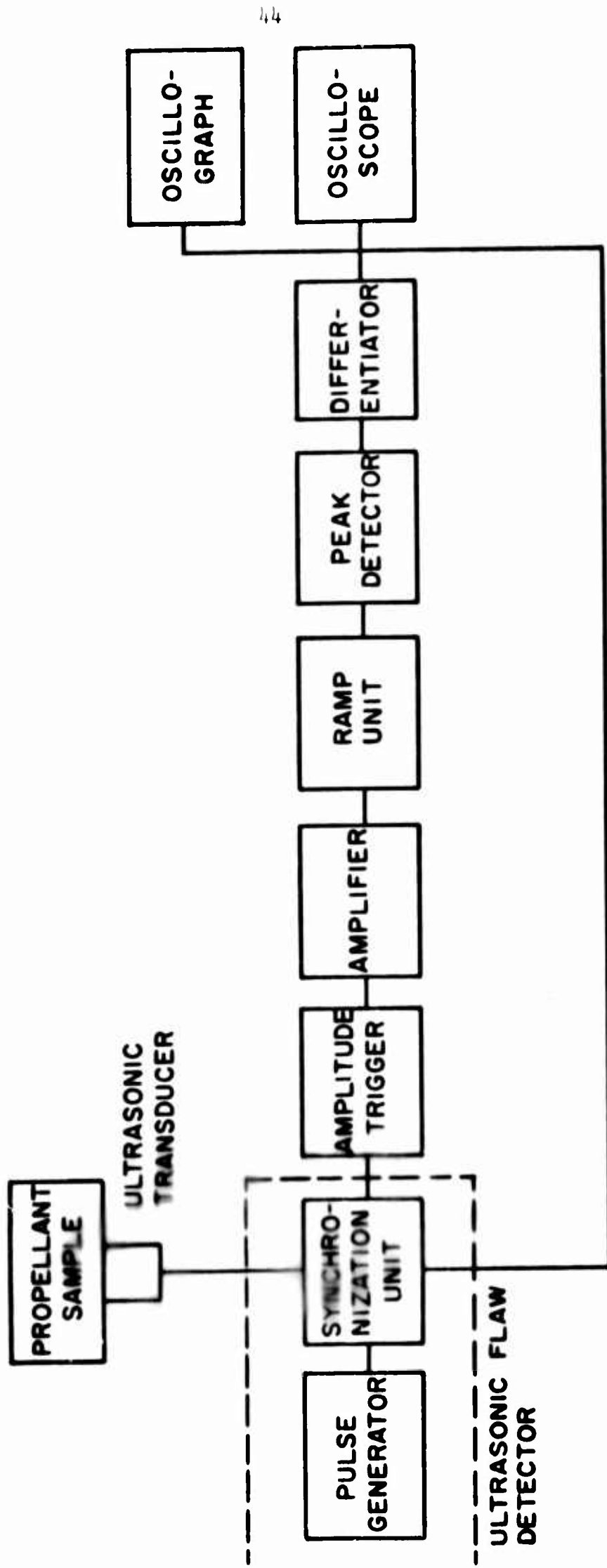be recorded directly by an oscillograph.

FIG. 9   ULTRASONIC TRANSDUCER OUTPUT

FIG. 10   MODIFIED ULTRASONIC SYSTEM

Status of the Ultrasonic Investigation

Currently, experiments are being conducted for determining an optimum ultrasonic frequency for non-burning samples of both aluminized and non-aluminized composite propellants. An optimum ultrasonic frequency for each type of propellant will provide for the desired attenuation in the amplitude of the echo-pulse.

After the optimum ultrasonic frequency has been determined, small samples of propellant will be fired in a two-dimensional research rocket motor which will incorporate the ultrasonic transducer. The data obtained by the ultrasonic technique will be compared with known burning rate data for the subject propellant.

Experiments will be conducted to determine the effects, if any, of the interaction of the propellant combustion zone and the ultrasonic pulses.

BIBLIOGRAPHY

BIBLIOGRAPHY

1. Murphy, J. M. "Technical Memorandum on the Current Status of Erosive Burning in Solid Propellant Rocket Motors," Report Number TM-62-6, Jet Propulsion Center, Purdue University, August, 1962, Confidential.

2. Osborn, J. R., Murphy, J. M., and Kershner, S. D., "Photographic Measurement of Burning Rates in Solid Propellant Rocket Motors," The Review of Scientific Instruments, March, 1963, pp. 305-306.

3. Osborn, J. R., and Burick, R. J., "Continuous Measurement of the Burning Rates of Solid Rocket Propellants," Report Number I-64-3, Jet Propulsion Center, Purdue University, April, 1964.

4. Osborn, J. R., and Panella, R. F., "Analysis of a Servo System for the Continuous Measurement of the Burning Rate of a Solid Propellant," Report Number I-64-4, Jet Propulsion Center, Purdue University, May, 1964.

5. Osborn, J. R., Burick, R. J., and Panella, R. F., "Continuous Measurement of Solid Propellant Burning Rates," Final Report Number F-64-3, Jet Propulsion Center, Purdue University, July, 1964.

6. Zucrow, M. J., Aircraft and Missile Propulsion, Vol. II, John Wiley and Sons, Inc., New York, 1958.

7. Bleuler, E., and Goldsmith, G. J., Experimental Nucleonics, Rinehart and Company, Inc., New York, 1952.

8. Zucrow, M. J., Osborn, J. R., Murphy, J. M., and Kershner, S. D., "Investigation of Velocity Upon the Burning Rate of Solid Propellants," Report Number F-63-3, Jet Propulsion Center, Purdue University, December 1963, Confidential.

9. Stone, M. W., "The Slotted-Tube Grain Design," Report No. S-27, Rohm and Haas Company, Hunstville, Alabama, December 23, 1960.

10. Barrow, G. M., Molecular Spectroscopy, McGraw-Hill Book Company, Inc., 1962.

11. Viegas, J. R., and Peng, T. C., "Electrical Conductivity of Ionized Air in Thermodynamic Equilibrium," ARS Journal, Vol. 31, No. 1 May, 1961.

12. Hayt, W. H. Jr., _Engineering Electromagnetics_, McGraw-Hill Book Company, Inc., New York, 1958.

13. Barrere, M., Jaumotte, A., DeVeubeke, B., and Vandenkerckhove, J., _Rocket Propulsion_, Elsevier Publishing Company, Amsterdam, 1960.

14. Francis, G., _Ionization Phenomena in Gases_, Academic Press Inc., New York, 1960.

15. Banks, B., Cldfield, G. E., and Rawding, H., _Ultrasonic Flaw Detection in Metal_, Iliffe Books Ltd, London, 1962.

16. Babikov, O. I., _Ultrasonics and its Industrial Application_, Consultants Bureau Enterprises, Inc., New York, 1960.

17. Goldman, R. G., _Ultrasonic Technology_, Reinhold Publishing Corporation, New York, 1962.

18. McClure, F. T., Hart, R. W., and Bird, J. F., "On Acoustic Resonance in Solid Propellant Rockets," Report No. TG 335-2, Applied Physics Laboratory, The Johns Hopkins University, Sept., 1959.

19. Redwood, M., "Problems in the Propagation of Ultrasonic Pulses in Solids," Ultrasonics, Vol. 2, Oct.- Dec., 1964.

APPENDICES

APPENDIX A

NOTATION

Servomechanism Technique

Symbol	Explanation	Units
E	Feedback signal statistical error	$\left[\dfrac{\text{Time}}{\text{Counts}}\right]^{1/2}$
$\bar{n}$	Nominal counting rate	Counts/Time
r	Burning rate	In/Sec
r_s	Velocity of propellant positions shaft	In/Sec
σ	Root mean square error	$\left[\dfrac{\text{Counts}}{\text{Time}}\right]^{1/2}$

Microwave Technique

Symbol	Explanation	Units
c	Velocity of light	cm/sec
e	Electron charge	coulomb
E	Electric field intensity	Volt/m
f	Microwave frequency	cps
f_{lm}	Mean frequency of quantum states l and m	cps
h	Planck's constant	erg/sec
i	Convective current	$\text{coulomb}/\text{m}^2$ sec
J	$J = \sqrt{-1}$	
k	Boltzmann constant	$\text{erg}/^{\circ}\text{K}$
K	$K = \omega\sqrt{\mu\epsilon}$	1/m

Symbol	Explanation	Units
M	Molecular weight	lb
n_i	Concentration of an ionized gas molecule	$1/cm^3$
n_o	Molecular concentration	$1/cm^3$
N	Avogadro's number	1/gm-mole
p	Gas pressure	mm Hg
t	Time	second
T	Temperature	^{o}K
V	Velocity of the electron	ft/sec
x	Degree of ionization $X = \dfrac{n_i}{n_o}$	
Z	Thickness of the combustion chamber	cm

Greek

α	Absorption coefficient	1/m
ϵ	Permissivity of the medium	farad/m
μ	Permeability of the medium	henry/m
ρ_o	Density	lb/ft^3
ρ_e	Charge density	$coulomb/ft^3$
σ	Electric conductivity of the medium	mho/cm
ω	Microwave radian frequency	1/sec
ω_p	Plasma radian frequency	1/sec
∇	Gradient operator $\bar{i}\,\dfrac{\partial}{\partial x} + \bar{j}\,\dfrac{\partial}{\partial y} + \bar{k}\,\dfrac{\partial}{\partial z}$	

Ultrasonic Technique

Symbol	Explanation	Units
C	Oscillograph recording speed	in/sec
f	Ultrasonic frequency	cps
I_i	Intensity of the incident wave	erg/cm^2
I_r	Intensity of the reflected wave	erg/cm^2
I_o	Initial intensity	erg/cm^2
I_x	Intensity at distance x	erg/cm^2
r	Burning rate	in/sec
V	Sonic velocity	cm/sec
X	Ultrasonic traveling distance	cm
Z	Specific acoustic impedence	$gm/cm^2 sec$

Greek

α	Absorption coefficient	1/cm
ΔS	Thiness change of the propellant	inch
Δt	Ultrasonic traveling time	sec
ΔL	Difference in the pulse-echo spans of two successive input pulses	inch inch
ρ	Density of the medium	gm/cm

APPENDIX B

DERIVATION OF THE GENERAL WAVE EQUATION

Maxwell's equations for a free space may be expressed as:

$$\nabla \cdot \bar{E} = \rho_e / e \tag{30}$$

$$\nabla \cdot \bar{B} = 0 \tag{31}$$

$$\nabla \times \bar{E} = - \mu \frac{\partial \bar{H}}{\partial t} \tag{32}$$

$$\nabla \times \bar{H} = \bar{I} + \epsilon \frac{\partial \bar{E}}{\partial t} \tag{33}$$

where $\bar{E}$ is the electric field intensity, $\bar{B}$ is the magnetic flux density, $\bar{H}$ is the magnetic field intensity, ρ_e is the change density, $\bar{I}$ is the convective current, and ϵ is the permissivity of the medium.

A convenient vector identity is:

$$\nabla \times \nabla \times \bar{E} = \nabla (\nabla \cdot \bar{E}) - \nabla^2 \bar{E} \tag{34}$$

However, taking the curl of eqn. 32 yields

$$\nabla \times (\nabla \times \bar{E}) = \nabla \times (- \mu \frac{\partial \bar{H}}{\partial t})$$

$$\nabla \times (\nabla \times E) = - \mu \frac{\partial}{\partial t} (\nabla \times \bar{H}) \tag{35}$$

Utilizing eqn. 33, eqn. 36 may be written as:

$$\nabla \times (\nabla \times E) = - \mu \frac{\partial}{\partial t} \left[\bar{I} + \epsilon \frac{\partial \bar{E}}{\partial t} \right]$$

$$= - \mu \frac{\partial}{\partial t} \bar{I} - \mu\epsilon \frac{\partial^2 \bar{E}}{\partial t^2} \tag{36}$$

Thus, by eqn. 34 the general form of the wave equation is:

$$\nabla (\nabla \cdot E) - \nabla^2 E = - \mu \frac{\partial \bar{I}}{\partial t} - \mu\epsilon \frac{\partial^2 \bar{E}}{\partial t^2} \tag{37}$$